communications engineering

A Nature Portfolio journal

Article

Article in Press

https://doi.org/10.1038/s44172-026-00817-y

Immersive and wearable bi-directional thermal rendering for physical and virtual interaction in augmented reality

Check for updates

Alexandra Watkins [1] ✉, Ritam Ghosh[2], Evan Chow[1] & Nilanjan Sarkar[2]

Augmented reality blends virtual content with the physical world, creating a challenge for thermal feedback: users must feel virtual temperature cues without losing dexterity or access to real-world thermal information. Here we show that a palm-mounted warm/cool thermal feedback prototype can address this challenge through three design considerations: indirect feedback that leaves the fingertips unobstructed, active thermal passthrough that senses and reproduces the temperature of contacted physical surfaces, and spatially and temporally varying thermal stimulation. Human-subject experiments show that indirect feedback preserves immersion and comfort despite reduced realism when visual contact occurs at the fingertips; thermal passthrough supports discrimination between real and rendered temperatures; and moving thermal patterns increase immersion and realism compared with static stimulation. These findings suggest that our design considerations are viable design strategies for AR thermal haptics, while also clarifying tradeoffs for applications that require precise realism versus broader immersive thermal experience.

Thermal sensations are an important part of everyday object interaction. Warmth and coolness help people interpret material properties, environmental conditions, comfort, and safety, such as when holding a hot beverage or touching a cold metal rail. These experiences are mediated by thermoreceptors in the skin, which detect changes in temperature and support material discrimination and behavioral responses[1]. In immersive systems, thermal feedback can therefore contribute to presence, interactivity, and realism by making virtual or augmented objects feel more consistent with the physical experiences they represent[2–4]. As immersive technologies are increasingly used in education, workforce training, healthcare, and industrial processes[5–7], the need for effective multisensory feedback has also increased. Prior work has shown that the fidelity of immersive feedback can influence learning outcomes, task efficiency, and user satisfaction[8–11]. Thermal feedback is one important component of this broader challenge, particularly in AR, where virtual and augmented objects must be perceived in relation to the physical surfaces, materials, and interactions that surround them.

AR introduces design constraints that differ from those of virtual reality (VR). AR systems overlay digital information onto the user's physical environment, allowing virtual content to be perceived and manipulated in relation to real objects and spaces[12,13]. In contrast to fully virtual environments, AR users may need to grasp actual tools, touch real surfaces, and maintain awareness of physical material properties while simultaneously receiving feedback from virtual elements. Thermal feedback for AR therefore requires more than adding temperature cues to the hand; it requires strategies that balance physical interaction, real-world thermal perception, and coherent virtual sensation. Although recent AR head-mounted displays provide increasingly sophisticated visual and auditory feedback[14], haptic and thermal feedback remain important for supporting the perceived presence of virtual objects and interactions[15–19].

Compared with force, vibration, and tactile feedback, thermal feedback remains relatively underexplored in immersive interfaces[2]. Existing systems demonstrate that thermal stimuli can improve realism and presence[1,20,21], and recent wearable or multimodal devices have incorporated thermal cues into gloves, rings, handheld devices, and actuator arrays[22–25]. These approaches show the value of thermal feedback, but they also reveal a design conflict for effective use in AR. Devices that cover the fingers or require handheld controllers[26] may interfere with grasping, manipulation, or natural thermal sensing of physical objects. Such compromises may be acceptable in fully virtual contexts, but they become more consequential when users must interact fluidly with both physical and virtual entities in the same workspace.

We believe these AR-specific constraints motivate three design considerations for thermal feedback, as demonstrated in the use case of Fig. 1. First, indirect feedback can relocate thermal actuation away from the fingertips to reduce interference with manual dexterity. Second, active thermal

[1]Mechanical Engineering, Vanderbilt University, Nashville, TN, USA. [2]Mechanical Engineering, Electrical and Computer Engineering, Computer Science, Vanderbilt University, Nashville, TN, USA. ✉e-mail: alexandra.watkins@vanderbilt.edu

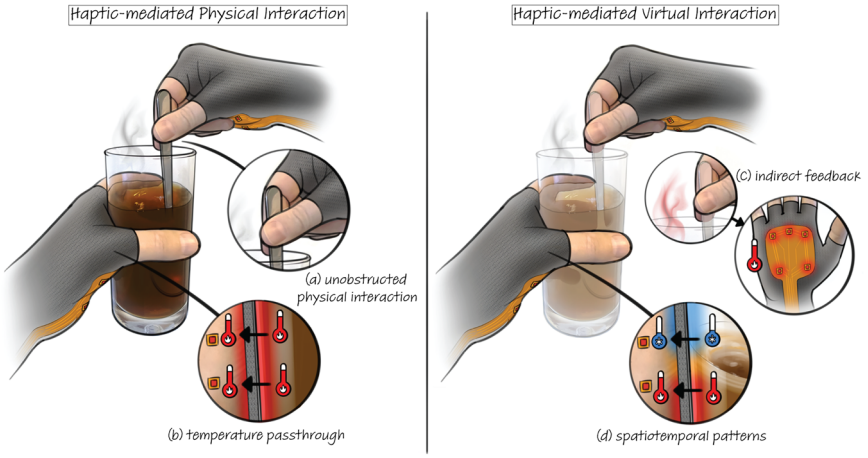


Fig. 1 | Haptic-mediated thermal interactions in AR enabled by the proposed design considerations. a *Physical interaction*. Leaving the fingers unobstructed supports fine manipulation of physical tools or objects and preserves direct thermal sensing at the fingertips. **b** *Active thermal passthrough*. Temperature sensors on the external surface of a haptic device allow collocated thermal actuators on the interior surface to render the thermal properties of contacted surfaces. **c** *Indirect feedback*. Thermal sensations applied to nearby occluded regions, such as the palm, can provide thermal cues during virtual interactions while avoiding actuation on the fingertips. **d** *Spatiotemporal rendering*. Independently controlled and spatially arranged thermal actuators enable sensations that vary across the contact surface and over time, such as the walls of a virtual cup being covered and uncovered by warm liquid.

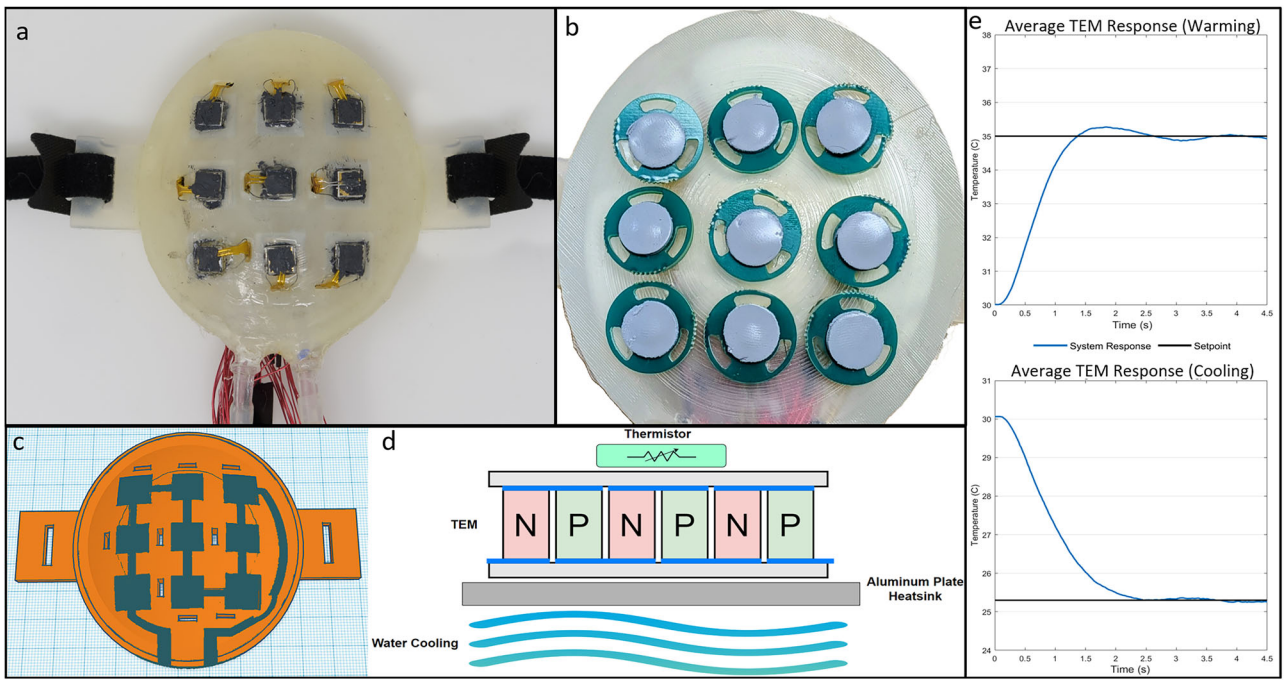


Fig. 2 | Overview of the proof-of-concept wearable thermal feedback system. a Thermal feedback is applied by an array of individually controlled Peltier devices with temperature feedback from thermistors mounted to each contact surface. **b** Outward-facing thermistors covered by a thermally conductive pad allow measurement of contacted surface temperatures for active thermal passthrough. Reflective phototransistors mounted on the bottom of each pcb allow for contact detection. **c** Interior to the silicone base is a water-cooling channel for temperature management. **d** A single thermal actuation unit consists of a thermoelectric module and thermistor mounted on an aluminum base that acts as a water-cooled heatsink. **e** Average temperature response to a step input while in contact with a human palm at an ambient temperature of 30 °C. Data for **e** is in Supplementary Data 1: TEM Response Times.

passthrough can address the loss of natural thermal sensing caused by device occlusion by actively measuring the temperature of contacted surfaces and rendering that temperature to the skin. Third, spatiotemporal thermal rendering can support thermal sensations that vary across the contact surface and over time, allowing virtual thermal events to better correspond to dynamic AR interactions. Together, these considerations frame thermal feedback for AR as a problem of balancing real-world touch, virtual object feedback, and mixed physical–virtual coherence.

In this manuscript, we present a proof-of-concept palm-mounted thermal-rendering prototype that implements these design considerations for AR (Fig. 2). The palm provides sufficient surface area for multiple thermal actuators while leaving the fingertips available for grasping, manipulation, texture perception, and direct contact with real objects. This form factor allows the device to explore indirect thermal feedback, active thermal passthrough, and spatially distributed thermal rendering without fully occupying the contact surfaces most often used for precise manual interaction. The system combines independently controlled thermoelectric modules (TEMs) with outward-facing contact-detection and temperature sensors to provide warm and cool sensations, active thermal passthrough, and time- and space-varying temperature sensations rendering on the palm using only thermal actuators.

We provide supporting evidence for our design considerations and their implementation in a proof-of-concept device using five controlled human-subject experiments. These experiments confirm the perceptual sensitivity to warm and cool stimuli on the palm as an appropriate location for haptic feedback, the user experience trade-offs of indirect feedback, the

ability of active thermal passthrough to support object temperature perception, recognition of spatial thermal patterns, and the effect of moving thermal rendering during AR interaction. This work contributes an AR-specific framing for thermal feedback, a wearable prototype implementation of three design considerations, and empirical evidence that these considerations can support thermal interaction while preserving the physical sensing and manual dexterity that distinguish AR from fully virtual environments. In particular, we demonstrate that the designed AR thermal interaction prototype for AR applications ensure immersion.

Results

Design considerations for AR thermal feedback

Thermal feedback for AR must balance virtual object rendering with continued interaction in the physical environment (Fig. 1). Unlike fully virtual systems, AR interfaces require users to grasp, manipulate, and thermally sense real objects while also perceiving temperature cues associated with virtual content. This creates a set of design tradeoffs: thermal cues must be perceptible and expressive, but the mechanisms used to render them should not substantially obstruct manual dexterity, interfere with physical contact, or eliminate access to real-world thermal information. These constraints motivate three design considerations for AR thermal feedback:

DC 1: Use indirect feedback to preserve manual dexterity.

DC 2: Use active thermal passthrough to preserve access to real-world temperature information.

DC 3: Use spatiotemporal rendering to support complex and dynamic virtual thermal interactions.

The first two considerations address how thermal feedback can coexist with real-world touch, while the third addresses how virtual thermal cues can vary across space and time to better match AR object interactions.

DC 1: use indirect feedback to preserve manual dexterity. A first consideration is whether thermal feedback can be delivered without occupying the fingertips, which are often needed for exploratory and manipulative touch in AR. Bhatia, Hornbæk, and Seifi[27] identified four types of touch interactions commonly used in AR from the set of exploratory procedures previously described by Lederman and Klatzky[28]. Three of these interaction types require the thumb or fingers. Directly mounting thermal actuators on these contact surfaces can therefore interfere with grasping, manipulation, and natural sensing of physical objects.

Indirect feedback addresses this issue by applying thermal cues to a nearby skin region rather than the apparent or functional point of contact. Prior work has explored displaced thermal stimulation at locations such as the base or back of the finger[29–31] and the wrist[32]. An additional candidate location explored by our prototype device is to use the palm as the indirect feedback site, as it provides a relatively large surface area for thermal actuation while leaving the fingertips available for precise physical interaction.

This approach introduces an important perceptual tradeoff. Relocating feedback away from the apparent point of contact may preserve dexterity, but it may also reduce realism if the visual and thermal locations do not align. This tradeoff is especially relevant because reducing actuator size or moving actuators away from the fingers can also limit heat transfer, contact area, and perceived stimulus intensity[33]. Thermal sensitivity varies across the body and depends on both absolute temperature and rate of temperature change[34–36]. By strategically positioning smaller, low-power actuators on areas with a higher thermoreceptor density or greater thermal sensitivity—the palm acting as a great example—we believe designers can maintain a significant thermal effect without sacrificing the user's dexterity or comfort.

DC 2: use active thermal passthrough to preserve access to real-world temperature information. The last type of common AR touch interaction identified by Bhatia et al.[27] is static contact and holding, where users maintain sustained touch with an object or surface. This method of interaction is particularly important for perceiving thermal properties of the environment, as humans intuitively use various regions of their skin, such as the palms, fingers, or even forearms, to gather thermal cues. However, when a thermal feedback device that requires contact is placed on these sensitive regions, it blocks direct contact with the physical environment. This creates a challenge: the user is no longer able to feel the true thermal characteristics of the object they are holding, potentially diminishing their sense of immersion and realism. Simply utilizing indirect feedback by itself does not adequately address this, as there is still the possibility that the area of skin occluded by the device is needed for intuitive interactions.

We propose a solution that we term *active thermal passthrough*: the device measures the temperature of a contacted physical surface using outward-facing sensors and renders a corresponding sensation to the skin using inward-facing actuators. This approach does not passively transmit the object's temperature through the device. Rather, it actively senses and recreates a device-mediated thermal cue. This introduces a tradeoff: active thermal passthrough can preserve access to real-world temperature information, but the rendered cue is necessarily mediated by sensor response, actuator dynamics, contact conditions, and the thermal properties of the device interface. Active thermal passthrough is therefore intended to reduce the loss of real-world thermal information introduced by the device itself, allowing users to retain access to contact-based temperature sensations while still benefiting from augmented thermal feedback.

DC 3: use spatiotemporal rendering to support complex and dynamic virtual thermal interactions. A third consideration is that virtual thermal cues may need to vary across both space and time. Real and virtual object interactions are rarely uniform: contact may occur over only part of the hand, the hand may move across a surface, or the thermal state of a virtual object may change during interaction. A single static thermal stimulus may therefore be insufficient for interactions in which the perceived contact location or temperature distribution changes over time.

Spatially varying thermal cues can contribute to the perception of surface properties and localized contact[37]. This need is consistent with exploratory procedures such as lateral motion and contour following, in which dynamic touch interactions reveal properties of textures, shapes, and surfaces[28]. Prior systems have demonstrated promising approaches to spatial thermal feedback, including benchtop thermal tactile displays[37] and wearable skin-like actuators[38]. However, spatial thermal rendering remains less explored in compact interfaces intended to support natural AR object interaction.

Temporal variation is also important when contact changes during motion. Existing approaches often combine a static thermal source with vibrotactile cues to create the illusion of moving heat or cold. This can rely on thermal referral, in which a stationary thermal stimulus appears to move when paired with shifting tactile stimulation[30,39,40]. Liu et al.[41] used this approach by overlaying static thermal output with moving tactile feedback, while Son et al.[42] developed a vest that combined vibrotactile and thermal actuators to render moving thermal sensations. Nakatani et al.[43] similarly combined a low-resolution grid of thermoelectric modules with a higher-resolution vibrotactile matrix to create a sense of thermal motion.

Thermal device design

We present a proof-of-concept wearable thermal feedback prototype designed to implement the three AR thermal feedback design considerations described above (Fig. 2). The device consists of an array of TEMs arranged in a 3 × 3 grid against the palm. Each module functions as an individual heat pump and can be independently controlled, allowing the device to support spatially and temporally varying thermal cues without additional modalities of feedback, as is typically done for thermal referral. A 10kΩ thermistor was attached to the active surface of each TEM for closed-loop temperature control. Each TEM–thermistor assembly was mounted on a 10mm × 10mm aluminum plate and embedded within a flexible silicone base. Internal water-cooling channels manage the temperature of the aluminum base

plates, which act as heat sinks and reduce thermal buildup during sustained operation.

To support active thermal passthrough, the outward-facing surface of the device includes a 3 × 3 grid of custom PCBs with a surface contact sensor (VCNT2020 reflective phototransistor) and a 10kΩ thermistor. Each thermistor is covered with a 0.2mm thermally conductive silicone pad to improve thermal coupling with contacted surfaces while protecting the sensor package. The phototransistor is mounted on the bottom of the custom PCB and registers contact when enough pressure is applied to close the air gap between the bottom of the PCB and the device's silicone body. Together, these outward-facing sensor modules allow the device to detect physical contact and measure contacted surface temperature, enabling active thermal passthrough when the palm is occluded by the device.

The device was mounted against the user's palm to operationalize indirect feedback while preserving the fingertips for grasping, manipulation, and direct physical contact. The palm remains near common fingertip interaction sites, can itself serve as a direct contact surface for virtual objects, and provides a relatively large area for rendering thermal sensations. Recent work has also shown that the palm can support the perception of thermal cues[35,44].

We make use of the large surface area of the palm by incorporating an array of 6.5mm × 6.5mm TEMs (CUI Device CP076581-238P) arranged in a 3 × 3 grid with 18mm spacing. Multi-actuator thermal arrays have been used in prior thermal rendering systems. Zhipeng et al.[45] developed a thermal display composed of a 3 × 3 set of heating actuators and a single TEM for cooling. More recently, Li et al. developed a wearable 4 × 4 array of thermoelectric actuators for hand rehabilitation after stroke[46]. Kim et al.[47] integrated a two-dimensional array of TEMs into the handle of a blind-assistive cane. These systems demonstrate the feasibility of array-based thermal rendering, but their use has primarily focused on non-AR or task-specific contexts rather than AR interactions that require simultaneous physical touch and virtual thermal feedback.

The individual modules are encapsulated within a flexible silicone base, which was selected for mechanical flexibility and biocompatibility. The flexibility and lightness of the material allow the device to be worn against the palm while limiting interference with fingertip contact. A two-part mold fabrication process was used to create internal water-cooling channels that disperse heat away from the TEMs and help maintain actuator efficiency during sustained operation. The current prototype remains tethered because of the external control circuitry and water-cooling reservoir. When strapped to the hand, the flexible base conforms to the palm surface, improving contact consistency between the thermal array and the skin and reducing positional slippage during movement.

Prototype characterization showed that the device's operational temperature range spans approximately 15 °C above and below the user's ambient skin temperature, with onset temperature change rates exceeding 0.1 °C/s within 50ms. The average delay from external-facing contact detection to actuation of the inward-facing TEMs against the palm was 5ms. Combining this contact-detection delay with the actuator response delay resulted in an estimated physical surface rendering delay of 55ms. This delay is below typical thermal sensing reaction times of the skin, which are on the order of 300–700ms [48,49]. A more detailed description of the device fabrication and performance characterization is provided in the Methods section.

Participants

Twelve (12) individuals from Vanderbilt University's undergraduate and graduate student populations were recruited for this study with approval from Vanderbilt's Institutional Review Board. Recruitment focused on participants who were available during the study's scheduled sessions and willing to take part. Prior to participation, each individual was provided with a detailed explanation of the study's purpose, procedures, potential risks, benefits, and their rights as participants. Written informed consent was obtained after participants had the opportunity to ask questions and receive clarification.

Each participant attended four sessions, lasting 1 h each, during which they completed the study's tasks and activities. This session length was chosen to balance data collection needs with minimizing participant fatigue or discomfort.

The participant group had a median age of 24.2 years with a standard deviation of 3.4 years. Most participants reported minimal or no prior experience with head-mounted display (HMD) VR/AR technology.

Experiment 1: JND testing

To characterize whether thermal changes rendered through the device were perceptible, we quantified the just noticeable difference (JND) for device-mediated thermal stimuli. The JND represents the smallest difference between a reference stimulus and a test stimulus that can be detected with a specified level of reliability. In this experiment, we defined the JND as the stimulus difference corresponding to a 75% probability that a participant would report the reference and test stimuli as different.

We used a one-up/one-down adaptive weighted staircase procedure with an asymmetric step-size to target the 75% detection threshold[50]. On each trial, participants were presented with a reference stimulus followed by a test stimulus. The test stimulus differed from the reference stimulus by an adjustable percentage offset. After each response, this offset was updated based on the participant's judgment. If the participant reported that the stimuli were different, the offset was decreased by 10%, making the next comparison more difficult. If the participant reported that the stimuli felt the same, the offset was increased by 30%, making the next comparison easier.

The adaptive staircase experiment was conducted for four total conditions: warming the entire thermal device, cooling the entire thermal device, warming a single row of the TEM array, and cooling a single row of the array. The bottom horizontal row of TEM elements in the device was chosen for the line conditions (Fig. 3a, b), which corresponds to testing the JND of the thenar eminence and base of the palm. The chosen conditions were selected to evaluate both the global and localized thermal sensitivity of the palm, as these areas are critical for perceiving thermal feedback in AR applications.

A reference stimulus of 4 °C above or below the device's ambient temperature (30 °C) was chosen for the heating and cooling trials, respectively. An initial step size of 4 °C was chosen, meaning the initial test stimulus was 8 °C above or below ambient conditions. Each stimulus was presented to the user for a period of 3.5 s, with no Inter-Stimulus Interval (ISI) between them (ISI=0s). No ISI was chosen to avoid time order errors, based on the results of Hojatmadani et al.[51], who found that ISI had a significant effect on calculated JNDs. Before and after the presentation of the two stimuli, the thermal device was allowed to return to its ambient temperature. Each staircase test was conducted until 10 reversals were observed (changes in response from same to different or different to same, see Fig. 3c). The step sizes at the last eight reversals were then averaged to calculate the participant's JND for the specific condition.

The results of the JND testing are shown in Fig. 3. The individual JNDs for each condition failed to reject the null hypothesis of the Shapiro–Wilk test, indicating that they come from normal distributions. As such, the individual JNDs for each condition were fit to a normal curve in order to derive the 95% Confidence Interval (CI). The "Line-Warming" condition was found to have an average JND of 3.88 °C (95% CI: 3.49–4.27 °C), the "Line-Cooling" condition to have an average JND of 3.75 °C (95% CI: 3.36–4.14 °C), the "All-Warm" condition to have an average JND of 2.51 °C (95% CI: 2.30–2.71 °C), and the "All-Cool" condition an average JND of 2.88 °C (95% CI: 2.54–3.22 °C). This is consistent with previous work by Hojatmadani et al.[51] investigating the JND of the human palm.

An ANOVA was run on all four conditions, and no significant difference was found among the conditions ($p = 0.0549$). However, the low p value gives weight to the observed trend that the JND was smaller for the "All" mode conditions, implying that users can detect a smaller threshold between presented stimuli when the entire TEM array is activated.

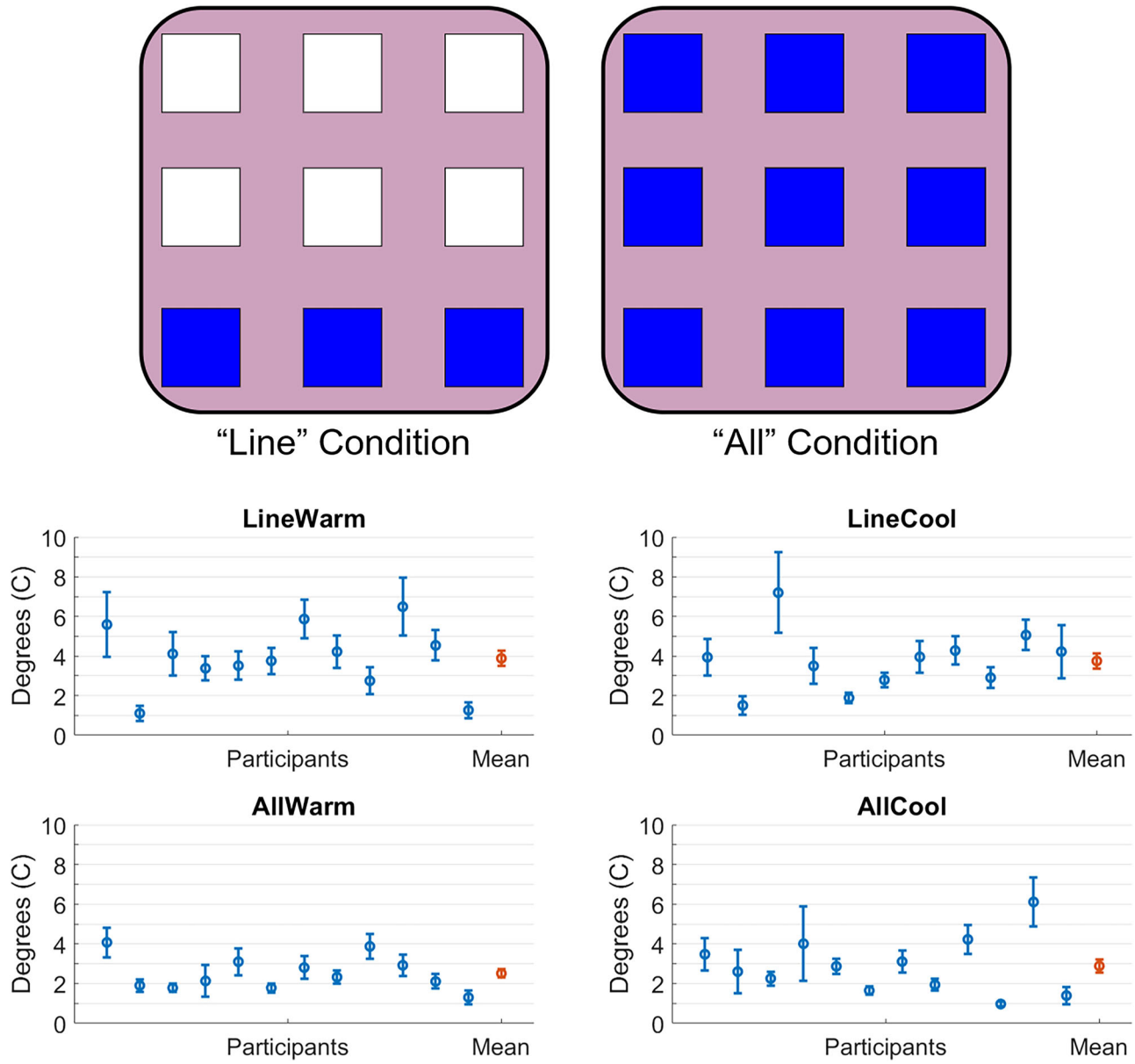


Fig. 3 | Just noticeable difference (JND) experiment conditions and results. Two distinct spatial patterns were applied to the device for both heating and cooling JND calculations for $n = 12$ participants. (*Line*) The "Line" pattern activated bottom row of TEMs on the device. (*All*) For the "All" pattern, all TEMs were activated. (*JND Results*) The JND (in degrees celsius) quantifies the smallest change in a reference temperature that is detectable with a 75% confidence. Per-participant JND is shown in blue and the overall JND is shown in orange. Error bars denote the 95% Confidence Interval. Data available in Supplemental Data 2: Human Subjects Data.

Experiment 2: user experience with indirect feedback

Although indirect feedback can preserve dexterity by leaving the fingertips unobstructed, this design choice requires that thermal cues delivered to the palm remain immersive during interactions that visually occur at the fingertips. It also requires that the mismatch between visual contact location and sensory feedback location does not increase user discomfort or decrease immersion. This experiment aims to validate *DC 1: Indirect Feedback* by evaluating whether thermal feedback applied to the palm can support fingertip-based virtual interactions without reducing the perceived quality of the experience.

Participants wore our haptic device and interacted with a virtual object (Fig. 4) set to either a warm or cool surface temperature. Each participant completed four trials: two fingertip interaction trials and two palm interaction trials. For each interaction location, one trial presented a warm stimulus and one presented a cool stimulus. The temperature setpoint for each trial was defined relative to the participant's skin temperature, with warm trials set to 8°C above skin temperature and cool trials set to 8 °C below skin temperature. Trial order was randomized within participants.

After completing all four interaction trials, participants answered three Likert-scale questions for both the fingertip and palm interaction conditions. Participants rated their sense of immersion, the realism of the thermal sensations, and their comfort during the interaction. Each question used a 1–7 scale, where 1 indicated no immersion, no realism, or maximum discomfort, and 7 indicated complete immersion, complete realism, or complete comfort.

Table 1 shows the results of the Likert-scale responses. Wilcoxon signed-rank tests were conducted to compare responses between the fingertip and palm interaction conditions. No significant difference in immersion was observed ($p = 0.119$), with an average rating of 5.83 for fingertip interactions and 6.13 for palm interactions. Comfort ratings additionally showed no significant difference ($p = 0.9999$), with an average score of 4.04 for fingertip interactions and 4.08 for palm interactions.

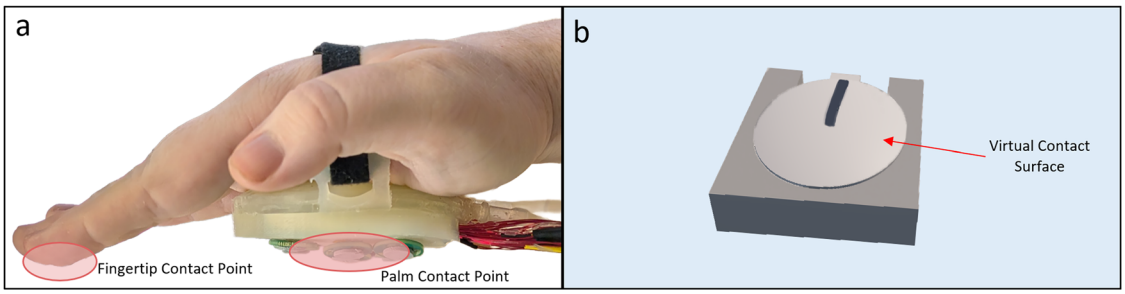


Fig. 4 | Indirect feedback experimental setup and results. a The fingertip and palm contact points utilized in this experiment. In both scenarios thermal sensations are applied via our device to the palm contact region. **b** The virtual object with an identifiable contact surface utilized for this experiment. Participants touched the central circular region with both their fingertips and palm.

Table 1 | Experiment 2 Likert scale results

	Fingertip	Palm	p
Immersion	5.83	6.13	0.119
Realism	2.88	6.17	1.5×10^{-5}
Comfort	4.04	4.08	0.9999

Results from a 7-point Likert scale with $n = 12$ participants measuring immersion, realism, and comfort. A two-sided Wilcoxon signed-rank test was used to determine significance. The observed mismatch between the fingertip and palm conditions in perceived realism ($p = 1.5 \times 10^{-5}$)), i.e. how accurate the sensations were compared to a real interaction, did not affect the comfort of the interaction ($p = 0.9999$) or its immersion ($p = 0.119$)), i.e. suspending disbelief to perceive the virtual object as actually being the sensed temperature. Data available in Supplemental Data 2: Human Subjects Data.

In contrast, realism ratings were significantly lower for fingertip interactions than for palm interactions ($p = 1.5 \times 10^{-5}$). Fingertip interactions received an average realism score of 2.88, while palm interactions received an average realism score of 6.17. These results indicate that participants perceived a clear reduction in realism when thermal feedback was delivered to the palm while visual contact occurred at the fingertips. However, this mismatch did not transfer to reduced immersion or increased discomfort. Participants remained immersed despite the reduced realism of the indirect feedback condition, and comfort ratings were neutral in both conditions.

Experiment 3: active temperature passthrough

No matter the choice of body placement of an AR indirect thermal feedback device, there will be an occluded area of skin the user cannot use for sensing their physical environment. This experiment validates *DC 2: Temperature Passthrough* by characterizing the efficacy and immersiveness of our thermal device's "temperature pass-through" capability. We conducted an object interaction experiment utilizing a test stand with a temperature-controlled surface (Fig. 5) and virtual replicas of the test stand. The test stand's contact area was made from 6061 aluminum CNC'd into a concave ellipsoidal surface. An embedded thermistor in the aluminum enabled closed-loop temperature control using a 45 mm× 45 mm TEM (ATS-TEC40-39-004) under the aluminum component. This assembly was then mounted onto a copper water-cooling heatsink for temperature management.

Participants were asked to compare the temperature of a pair of objects and state whether the objects were at equal or different temperatures. Table 2 presents the tested conditions. The "Real vs Virtual" trials asked participants to wear the device on their right hand and compare the test stand's temperature against a virtual replica of the test stand. The "Bare vs Device" trials involved just the physical test stand; participants first touched the test stand with their bare left palm and then again with the haptic device equipped on their right palm. The bare left palm was used to avoid the long delays that would have been required to repeatedly mount and dismount the thermal device on the right hand.

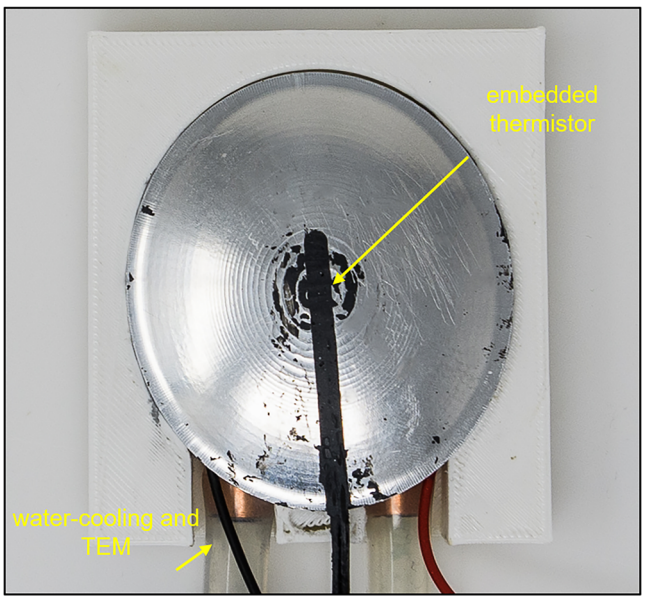


Fig. 5 | Temperature passthrough experimental setup, conditions, and results. A convex aluminum surface with an embedded thermistor sits atop a thermoelectric module and heatsink to act as a temperature-controlled surface.

Table 2 | Active temperature passthrough conditions

Condition	Comparison type	Temperature	# Trials
RV-W	Real vs Virtual	Warm	3
RV-C	Real vs Virtual	Cool	3
BD-W	Bare vs Device	Warm	3
BD-C	Bare vs Device	Cool	3
Total Trials Per Participant			12

$n = 12$ participants performed 3 trials for each of the four identified conditions.

Each of the four conditions shown in Table 2 included three trials. In one trial, both object interactions were set to the same temperature offset of 5 °C from the participant's skin temperature: a positive offset for Warm conditions and a negative offset for Cool conditions. For another trial, one object interaction had an offset of 5 °C and the other 10 °C, and in a third trial, object interactions had offsets of 5 °C and 15 °C.

The order in which each condition was tested was randomized between participants, and the order of the three temperature offset configurations was randomized within each condition. A 3 s delay was enforced between each trial's two object interactions so that the real test stand had sufficient time to change its surface temperature during the "Bare vs Device"

Table 3 | GLME fixed effect summary

		Response accuracy		$\beta_{log-likelihood}$		
Fixed Effect	Condition	Mean(%)	95% CI	Mean	95% CI	p
Base (Intercept)	RV-W	94.8	88.3–97.74	2.89	2.02–3.77	1.07^9
Temperature	RV-C	95.4	80.5–99.0	0.13	−0.60–0.87	0.721
Comparison Type	BD-W	87.2	57.2–97.2	−0.98	−1.73—0.22	0.012
Interaction Term	BD-C	93.0	52.3–99.7	0.54	−0.21–1.28	0.155

A Generalized Linear Mixed Effects model was employed to test significance between conditions in data from $n = 12$ participants. Overall device accuracy is shown in the Base(Intercept) effect ($p = 1.07^9$). Warm vs Cool had no impact on accuracy ($p = 0.721$), and bare-handed vs device use had a significant impact on accuracy ($p = 0.012$). There was no significant interaction effect ($p = 0.155$). Statistical significance of fixed-effect coefficients was assessed using two-sided t-tests as implemented by Matlab's fitglme function. Reported p-values are unadjusted for multiple comparisons. Data are presented as mean values with 95% confidence intervals. Data available in Supplemental Data 2: Human Subjects Data.

condition. At the end of this experiment, participants were asked to rate the overall realism of the object interactions during the AR experience using a Likert-scale of 1–7, with 1 being completely unrealistic and 7 being completely realistic.

To account for participant-level variation and within-subject temperature offset variation, a Generalized Linear Mixed Effects (GLME) model was used to predict response accuracy. Fixed effects included the warm vs cool condition and the type of comparison being made ("Real vs Virtual" or "Bare vs Device"). Random effects were participant and temperature offset. A logit link function was employed as both predictors were ordinal. Significance of the Likert-scale realism score was tested using the Wilcoxon signed-rank test. Post-hoc binomial tests were conducted to calculate response accuracy p-values.

Table 3 shows the results of fitting the GLME model. Fixed effects showed that the warm vs cool condition had no significant effect on accuracy ($p = 0.721$), while the bare-handed vs purely haptic predictor was significantly associated with accuracy ($\beta_{log-likelihood} = -0.976$, $p = 0.012$). This effect can be seen in its average response accuracies, with the overall accuracy of the haptic device at 94.8% ($p = 1.07^9$). No significant interaction effect was observed. Realism scores had an average value of 5.75 ($p = 9.77 \times 10^{-4}$), indicating that participants experienced a moderate degree of realism.

Experiment 4: spatial patterns

To begin validating *DC 3: Spatiotemporal Patterns*, we first evaluated participants' spatial discrimination accuracy. We developed a spatial pattern discrimination task in which participants were presented with one of six predefined patterns: the left, right, or middle vertical column of the array, or the top, bottom, or middle horizontal row of the array. After a brief period of exposure, the pattern either transitioned to another pattern from the set or continued to present the same thermal pattern. Participants were asked to report whether they noticed any change in the spatial profile of the thermal sensation applied to their palm. This process was conducted for every combination of pattern pairs from the set, for both warm and cool stimuli.

A temperature step size of 8 °C above or below skin temperature was used for the presentation of thermal patterns. This was chosen to be well above the JNDs measured in the first experiment to ensure that discrimination was not limited by insufficient temperature differences. Each pattern was applied to the participant for 3 s before either transitioning to the second pattern for 3 s or maintaining the current pattern for an additional 3 s. The thermal device then returned to ambient skin conditions. A total of 60 trials were conducted with each participant: 15 trials with a spatial pattern transition and 15 trials without a transition, for both the warm and cool conditions.

The results of the spatial pattern discrimination task are shown in Fig. 6. Accuracy in detecting pattern changes ranged from 41.7% to 100% for warm stimuli and from 50.0% to 100% for cool stimuli. The warm condition had an overall transition detection accuracy of 77.8%, while the cool condition had an overall transition detection accuracy of 78.9%. There was no significant difference in responses between the warm and cool conditions ($p = 0.9999$).

We also evaluated whether spatially rendered thermal feedback could support immersive virtual object interactions. Participants were asked to press their palm against a virtual replica of the temperature-controlled test stand used in Experiment 3, with the hand positioned such that approximately half of the palm contacted the virtual object and the remaining half extended beyond either the left or right side of the object. When combined with hand tracking, this interaction activated either one or two rows of the thermal array depending on variation in hand placement. Each participant experienced this interaction twice: once with a warm stimulus set to 8 °C above skin temperature and once with a cool stimulus set to 8 °C below skin temperature. The order of warm and cool stimuli and left- and right-sided placement of the palm were randomized within participants.

After completing both interactions, participants answered the same Likert-scale questions on immersion and realism used in Experiment 2, shown in Table 4. Single-sample Wilcoxon Signed Rank tests were used to evaluate whether the ratings were significantly different than the neutral midpoint of the scale. Participants reported an average immersion score of 6.04 ($p = 1.32 \times 10^{-5}$) and an average realism score of 5.83 ($p = 3.02 \times 10^{-5}$), indicating that spatially rendered thermal feedback supported both immersive and realistic object interactions. These ratings were not significantly different from the palm interaction ratings in Experiment 2 for either immersion ($p = 0.617$) or realism ($p = 0.135$) (Table 1), suggesting that spatially constrained thermal rendering preserved the perceived quality of direct palm-based feedback.

Experiment 5: moving thermal rendering in AR

To finish validation of *DC 3: Spatiotemporal Patterns*, a final experiment was conducted to evaluate immersion and realism during a dynamic spatiotemporal AR object interaction (Fig. 7). While still wearing the device, participants were asked to place their right palm to the left of — and level with the surface of — a virtual replica used in previous experiments of the temperature-controlled test stand used in Experiment 3. Participants were then asked to brush their palm laterally from left to right across the surface of the virtual object until their palm was positioned to the right of the object. They were instructed to perform this brushing motion at a slow pace, with approximately 3 s elapsing from initial contact on the left side of the virtual surface to the end of contact on the right side. The motion and speed were demonstrated by study personnel for each participant before they were asked to perform the action.

Two thermal rendering conditions (Fig. 7) were tested: a static thermal stimulus and a moving thermal stimulus. In the static condition, thermal feedback was applied to the palm by activating the TEMs at the center and four corners of our haptic device's array when the participant's palm made contact with the virtual object's surface and deactivating the TEMs when contact stopped. In the moving condition, TEM actuators in the array were dynamically activated based on hand tracking and the estimated overlap between the participant's palm and the virtual object, creating a spatially varying thermal pattern as the hand moved across the surface. Participants

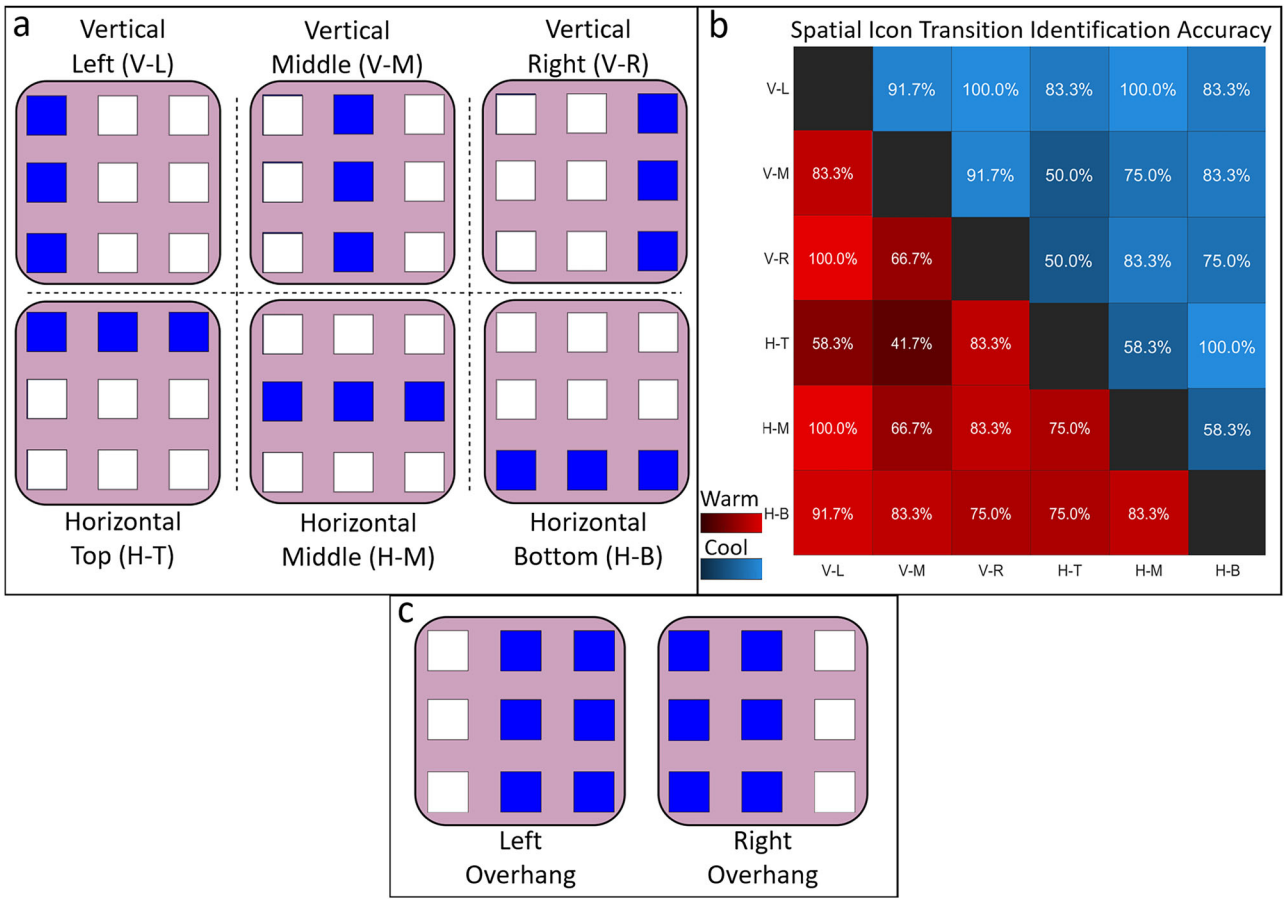


Fig. 6 | Spatial patterns experimental setup and results. a Transitions between six spatial patterns that utilized the device's 3 × 3 TEM grid were applied to participants wearing the device, for both warm and cool sensations. **b** The reported discrimination accuracy for each pattern pair transition are shown in the matrix heatmap. **c** The thermal patterns corresponding to the participant's palm overhanging the left or right side of the virtual object. Data for **c** available in Supplemental Data 2: Human Subjects Data.

Table 4 | Experiment 4 Likert scale results

	Mean	*p*
Immersion	6.04	1.32×10^{5}
Realism	5.83	3.02×10^{5}

Results from a 7-point Likert scale with $n = 12$ participants. A two-sided Wilcoxon Signed Rank test was used to determine significance ($p_{immersion} = 1.32 \times 10^{-5}$, $p_{realism} = 3.02 \times 10^{5}$. Data available in Supplemental Data 2: Human Subjects Data.

were able to experience each condition once with a warm stimulus set to 8 °C above skin temperature and once with a cool stimulus set to 8 °C below skin temperature. The order of warm and cool stimuli was randomized within participants.

After completing the interaction trials, participants answered Likert-scale questions on immersion and realism for both the static and moving thermal rendering conditions (Table 5). The Wilcoxon Signed-Rank test was again utilized for analysis. The moving thermal rendering condition produced significantly higher ratings than the static condition for both immersion ($p = 1.42 \times 10^{-4}$) and realism ($p = 1.49 \times 10^{-5}$). Average immersion increased from 5.13 in the static condition to 6.42 in the moving condition, while average realism increased from 3.46 in the static condition to 6.13 in the moving condition.

These results indicate that spatiotemporal thermal rendering improved the perceived quality of dynamic AR object interactions. Compared with a static stimulus applied to the center of the palm, thermal feedback that moved across the array in correspondence with hand-object overlap produced higher immersion and realism, supporting the use of spatially and temporally varying thermal patterns for rendering contact with virtual surfaces.

Discussion

We developed and evaluated a palm-mounted thermal feedback prototype for augmented reality that integrates active heating and cooling, real-time temperature sensing, and independently controlled spatial thermal rendering. The device was designed around three AR-specific design considerations: preserving manual dexterity through indirect feedback, maintaining access to real-world temperature information through thermal passthrough, and rendering spatially and temporally dynamic thermal cues for virtual object interactions. Across five controlled human-subject experiments, the results provide evidence that palm-mounted thermal feedback can support immersive AR interactions while preserving important aspects of real-world touch.

Indirect feedback and the tradeoff between dexterity and realism

Experiment 2 demonstrates an important distinction between immersion and realism in indirect thermal feedback. Delivering thermal feedback to the palm while visual contact occurred at the fingertips significantly reduced perceived realism, indicating that participants recognized the mismatch between where the interaction appeared to occur and where the thermal sensation was felt. However, this mismatch did not significantly reduce immersion or increase discomfort. This suggests that exact colocation of thermal feedback may not be necessary for every AR interaction.

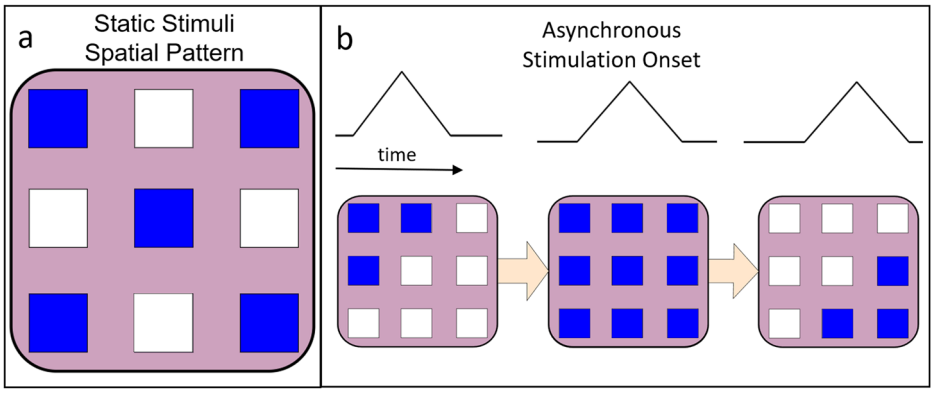


Fig. 7 | Moving stimuli experimental setup and results. a A static cross-shaped pattern was used at the control condition for this experiment. **b** An example depiction of a moving spatiotemporal pattern created by the asynchronous activation of TEMS as the user's hand and haptic device move laterally across a virtual surface.

Table 5 | Experiment 5 Likert scale results

	Static Stimuli	Moving Stimuli	*p*
Immersion	5.125	6.42	1.42×10^{-4}
Realism	3.46	6.13	1.49×10^{-5}

Results from a 7-point Likert scale with $n = 12$ participants. A two-sided Wilcoxon Signed Rank test was used to determine significance ($p_{immersion} = 1.42 \times 10^{-4}$, $p_{realism} = 1.49 \times 10^{-5}$). Data available in Supplemental Data 2: Human Subjects Data.

This finding has practical implications for wearable thermal device design. Fingertip-mounted devices can provide spatially congruent feedback, but they also interfere with the same contact surfaces that users rely on for grasping, manipulation, and texture exploration. Palm-based indirect feedback can be a valid design alternative: it preserves the fingertips for natural interaction while still providing thermal cues that can support the user's sense of engagement with the virtual environment. The reduced realism observed in the fingertip condition indicates that this approach is not equivalent to direct fingertip feedback. However, the preserved immersion suggests that users may tolerate this sensory displacement when the goal is to enhance the general sense of immersion in an AR experience rather than perfectly reproduce fingertip contact. This distinction is also particularly relevant for AR applications where users frequently transition between real and virtual interactions. In these scenarios, preserving manual dexterity may be more important than achieving perfect sensory colocation. Conversely, applications requiring precise fingertip realism, such as fine material discrimination or high-fidelity manual training, may require either fingertip feedback or a hybrid approach that combines direct and indirect stimulation. Together, these results support *DC 1: Indirect Feedback* by showing that thermal feedback can be relocated away from the apparent point of contact without reducing immersion or increasing discomfort.

Active thermal passthrough and preserving real-world interaction

The passthrough results support the value of treating occlusion as a primary design problem for AR haptics. Any wearable device placed on the hand blocks some portion of natural tactile and thermal perception. For a palm-mounted thermal device, this is especially important because the palm is often used for sustained contact with objects and surfaces. Without passthrough, the device would improve virtual interaction while degrading physical interaction, undermining the central goal of AR: blending virtual content with the real world.

Experiment 3 indicates that temperature passthrough can restore a substantial portion of the thermal information lost when the palm is covered by the device. Participants were able to distinguish temperature differences with high accuracy when comparing physical and rendered thermal stimuli, and the reported realism scores suggest that the rendered sensations were perceptually convincing during object interactions. The lower performance in the Bare vs Device comparison, relative to device-mediated comparisons, also shows that passthrough does not fully reproduce bare-skin sensing. This is expected because the device inserts several stages between the object and the user: external temperature sensing, control logic, actuator response, heat transfer through the TEM interface, and contact with the skin.

The implication is not that passthrough eliminates the perceptual cost of wearing a device, but that it can reduce this cost enough to preserve usable thermal interaction with the physical environment. This is an important design direction for AR haptics. Rather than choosing between augmenting virtual objects and preserving real-world touch, future devices can actively mediate between the two.

These results support *DC 2: Temperature Passthrough* by showing that thermal passthrough can preserve meaningful access to real-world temperature cues even when the skin is physically occluded by a wearable device. While passthrough does not fully reproduce bare-skin perception, it provides a practical mechanism for maintaining thermal interaction with physical objects while still allowing the device to render augmented or virtual thermal feedback.

Spatial and spatiotemporal rendering

Experiment 4 showed that participants were able to detect transitions between spatial thermal patterns at rates consistent with previous studies involving stationary thermal arrays[44,52]. This suggests that even a low-resolution thermal array can display spatial cues that extend beyond simply rendering the bulk thermal properties of an object. The ability to discriminate between thermal patterns supports the use of selectively activated regions of the TEM array to represent partial or irregular contact with a virtual object. For example, if a user touched a virtual cup partially filled with hot liquid, only the portion of the palm aligned with the filled region would need to be stimulated. The high immersion and realism ratings observed during the spatial rendering task further suggest that this type of spatially constrained feedback can preserve the perceived quality of palm-based thermal interaction.

Experiment 5 extended this concept to dynamic contact. When participants brushed their palm across a virtual surface, moving thermal feedback based on hand-object overlap produced significantly higher immersion and realism than a static stimulus applied to the center of the palm. This supports the idea that spatiotemporal thermal patterns can improve AR interactions by making the rendered feedback correspond to both contact location and hand motion. Rather than only indicating that a virtual object is warm or cool, the device can update the location of thermal stimulation as the interaction unfolds.

Together, these results support *DC 3: Spatiotemporal Patterns* by showing that spatially and temporally varying thermal cues can contribute to more immersive and realistic AR object interactions. They also suggest that dynamic thermal effects can be produced using thermal actuation alone, without requiring an additional vibrotactile modality to imply motion.

Design implications for AR thermal haptics

A central implication of these findings is that thermal feedback in AR should not be treated only as a question of actuator performance or maximum temperature range. Instead, the effectiveness of a thermal haptic system depends on how well the device fits within the user's broader interaction context. In AR, the user must continue to manipulate physical objects, sense real-world surfaces, and maintain perceptual coherence between physical and virtual elements. The results of this work suggest that these requirements can be addressed through a combined approach: relocating thermal feedback away from dexterous contact regions, restoring occluded thermal information through passthrough sensing, and dynamically rendering thermal patterns that correspond to virtual contact geometry and motion.

While indirect feedback is viable, its role should be chosen carefully. It can preserve immersion and comfort while maintaining manual dexterity, but it may reduce realism when the apparent contact point is far from the stimulated skin region. Designers should therefore use indirect thermal feedback when the benefit of leaving the fingers or other critical body part unobstructed outweighs the need for exact sensory colocation.

For AR applications, passthrough should be considered a core requirement for wearable thermal devices that cover thermally sensitive areas of skin. A device that only renders virtual temperature cues risks degrading the user's ability to perceive the real environment. By sensing and reproducing contacted surface temperatures, passthrough allows the device to serve both as an augmentation tool and as a compensatory interface for the skin it occludes.

Finally, spatial and temporal rendering should be prioritized, not constrained by device size or design complexity. Strong, static thermal stimuli may be easier to produce and control, but they do not necessarily improve coherence with AR interactions. The results from Experiments 4 and 5 suggest that thermal feedback becomes more compelling when it corresponds to contact location, object geometry, and hand motion. This points toward rendering strategies that are contact-aware rather than stimulus-only: the device should not merely output a target temperature, but should determine where, when, and how that temperature should appear on the hand.

Limitations and future work

Although wearable, the current prototype remains tethered to bench-top control electronics and a water reservoir, constraining user mobility to a tabletop workspace. Future iterations should integrate temperature management solutions onto the forearm, potentially via phase-change cooling methods[53], to aid portability. If water-cooling or other fluid-based cooling continues to be necessary, a possible space-saving technique could be the removal of a bulky fluid reservoir and instead relying on heat exchange between fluid in the system's tubing and the skin of the user's forearm. Combining such a human skin heat-exchange method with new advances in wearable technology for human thermoregulation[54] could avoid issues with localized temperature discomfort. Full portability could then be achieved by relocating heavy and bulky items such as batteries and control circuitry to a harness, belt, or backpack attached to the user's torso, with minimal cabling extending to the primary device on the palm and forearm.

Additionally, uneven contact pressure across the thermoelectric array produced variability in response times. Attempts were made to allow the TEM array to contour to the palm by using a flexible silicone material and molding it to have a convex shape. Yet it is apparent by looking at the system response of individual TEMS (See "Device performance") that not all TEMs exhibited the same thermal response times and damping/underdamping behavior when in contact with the palm. Contact pressure has long been known to affect thermal resistance between an object and human skin[55–57]. A variable contact pressure then affects the heat flow out of a TEM and into the surrounding skin. This means that a set of PID gains for temperature control for one set of TEMs will not be appropriate for another set with a different average contact resistance. A more efficient way of applying even contact pressure is needed, or a method of determining thermal contact resistance and adjusting individual PID gains accordingly.

In conclusion, this work provides evidence supporting the three proposed design considerations for thermal feedback in AR. Indirect feedback can preserve manual dexterity while maintaining immersion, thermal passthrough can reduce the perceptual cost of occluding the skin, and spatiotemporal rendering can improve the realism of virtual object interactions by aligning thermal cues with contact location and motion. Taken together, these findings suggest that effective AR thermal haptics require more than the addition of temperature cues; they require feedback strategies that intentionally balance physical interaction, real-world thermal perception, and coherent virtual sensation.

Methods

IRB approval

This research study underwent ethical review and was approved by the Vanderbilt University Medical Center Institutional Review Board (IRB) prior to its initiation (IRB #221508). The purpose of the IRB review is to ensure the protection of human participants involved in the research and to ensure compliance with ethical guidelines and regulations in accordance with the Declaration of Helsinki.

AR hardware and development software

All AR testing was performed with the HoloLens 2 headset. The AR scenarios used in experiments 1 through 4 were developed using Unity 2020.3.34f1 and the Microsoft Mixed Reality Toolkit (MRTK) v2.8.3.

The thermal haptic device was fabricated using a three-layer silicone structure, each layer serving a specific function. The top layer, which made direct contact with the user's palm, was designed to accommodate the TEMs and heat sinks. The middle layer incorporated water channels for cooling the cold side of the TEMs and provided attachment points for the Velcro strap used to secure the device to the user's hand. The bottom layer provided space for wire management and included dedicated slots for the thermistors, which measured the temperature of the real-world objects with which the user interacted.

Each silicone layer was molded using two-part silicone and fabricated in a two-part 3D-printed mold. These layers were cast separately and bonded with silicone-compatible CA glue. The heatsinks were inserted into the slots in the top silicone layer and attached with CA glue, and the TEMs were attached to the heatsinks using thermally conductive epoxy. The same epoxy was also used to affix a thermistor on top of each TEM to provide control loop feedback. Thermistor slots were strategically positioned in the bottom layer directly below each TEM to provide a one-to-one mapping of the TEMs with each external thermistor. This allowed the device to achieve "thermal passthrough" and pass on the temperature measured from the external object to the user's palm without loss of spatial resolution.

Thermoelectric modules

A thermoelectric module, also known as a Peltier device, creates heat flux across the junction of two dissimilar materials. When a DC electric current flows through the device, a temperature differential arises across the module as heat is transferred from one side to another, creating a "hot" side and a "cold" side, shown in Fig. 8a. The direction of heat flow is reversible by changing the direction of current flow through the TEM, meaning that a single contact surface can be used for both heating and cooling an object. This is important to keep in mind as the terms "hot" and "cold" are used to reference specific surfaces of the TEM, regardless of the direction of the temperature gradient. Convention is to designate the temperature-controlled surface as the "cold" side, with the "hot" side then being used for thermal management.

Heat absorption on the "cold" side of the device (q_{pel}) is a function of component materials, current temperature (T_c) and applied current (I):

$$q_{\mathrm{pel}} = -\alpha T_c I \tag{1}$$

where α is the Seebeck coefficient of the device, a term that encapsulates material properties, and the negative sign represents heat flow *out* of the

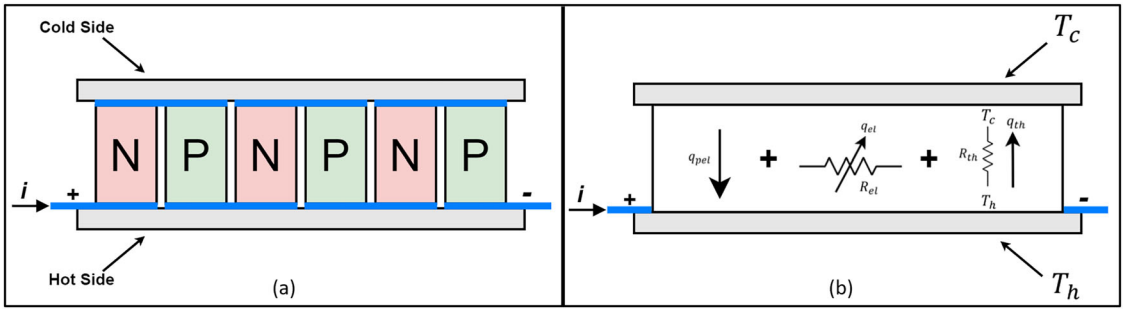


Fig. 8 | Thermoelectric module overview. a A thermoelectric device is made from alternating n- and p-type semiconductors placed in series electrically but in parallel thermally. When a DC current is passed through the semiconductors, a hot and cold side develop. **b** This temperature differential is due to heat flow from the Peltier effect, q_{pel}, and is resisted by electrical waste heat generation, q_{el}, and natural heat conduction, q_{th}.

"cold" side. This heat absorption is impeded by two additional effects: natural heat conduction back to the "cold" side due to the temperature differential, and waste heat generated due to the device's internal resistance and applied current.

Actual heat flow out of the "cold" side is more accurately described using the components of Fig. 8b in the following equation:

$$q_c = -\alpha T_c I + \frac{1}{R_{\text{th}}}(T_h - T_c) + \frac{1}{2}R_{\text{el}}I^2 \quad (2)$$

where R_{th} and R_{el} represent the device's thermal and electrical resistances, respectively. Only half of the electrical heat generated, $R_{\text{el}}I^2$, is included, as it is assumed waste heat is dumped equally on both sides of the module. The last two terms describing thermal conduction and waste heat have an important ramification: as the temperature differential across the device rises a decreasing amount of heat is effectively moved and the module becomes less efficient. There comes a point where natural heat conduction and waste heat generation completely negate the heat flow induced by the thermoelectric effect and the "cold" side temperature begins to rise, defining a maximum ΔT that can be generated across the device. If the "hot" side of the device is held near ambient conditions using a heat sink or other thermal management solution, this maximum temperature differential describes the bounds of simulated thermal sensations that can be applied to the skin contacting the device.

Control architecture

Special consideration must be given to the control hardware used with a TEM. Voltage regulation using an H-Bridge circuit controlled with pulse-width modulation (PWM) has a negative impact on the TEM's efficiency due to excessive waste heat generation. As described in Eq. (2), this is because the waste heat generated scales quadratically with applied current while thermoelectric heat flux is only linearly proportional to current. A PWM controller works by rapidly switching between a constant DC voltage and a grounded input. This method works well for loads with an inductive component, such as a motor, as the resulting current across the load is effectively steady and scales with the PWM's duty cycle. A TEM, on the other hand, is a purely resistive load, meaning that the induced current rapidly switches between a max value and zero amps, amplifying the waste heat losses. The solution to this problem is to filter the TEM's power source to generate a variable DC voltage supply with as little ripple voltage as possible. This can be implemented using a differential filter or a class D amplifier, but is more easily achieved by utilizing off-the-shelf TEM drivers and additional passive components to complete the filtering circuit.

The thermal display control loop we developed consists of a software PID controller, the ADN8833 TEM driver IC, a differential filter with a cutoff frequency of 5 kHz, and a thermistor mounted on the TEM's cold side for temperature feedback. Activation and temperature setpoints of TEMS during active temperature pass-through were controlled for each individual TEM by a corresponding surface contact and temperature measurement module, shown on the device in Fig. 2 and further detailed in Fig. 9. While the drive circuit, filter, and temperature and contact sensors are separate channels and contain unique hardware for each TEM, a single micro-controller is sufficient to run all the PID controllers and interface with a PC to receive thermal rendering input. Additional components of the control PCB include separate multiplexers for the thermistor readings, TEM current sense, and TEM voltage sense, allowing each to be read by the micro-controller using a single input pin each.

Water cooling

The fact that a TEM acts as a resistive load leads to a large amount of excess heat generation. In fact, the resistive heating dumped on the cold side ($\frac{1}{2}I^2R$) can sometimes approach Q_{max}, the maximum heat transfer capability of the TEM. Additionally, as described in Eq. (2), when in cooling mode, natural thermal conduction within the TEM transfers heat from the hot side to the cold side. If not addressed, this heat buildup will quickly counter any attempts to lower the temperature of the TEM's cold side. To address this issue, we added aluminum heatsinks to the hot side of the TEM and implemented a water-cooling solution to cool the heatsinks, composed of water channels built into the flexible and wearable silicone base itself, allowing for water cooling to be applied while still maintaining the mobile benefits of the wearable device already described. As seen in Fig. 2c, d, each TEM assembly is water-cooled in series, allowing for steady volumetric flow across each TEM.

When implementing the water-cooling solution, it was first necessary to determine the maximum total energy transfer that the water cooling solution would need to handle. This maximum necessary heat dissipation occurs when the TEM is in cooling mode, meaning the cold side is reduced in temperature and the hot side is increased in temperature. Flipping the signs of the q_{pel} and thermal conduction components in Eq. (2), we arrive at the following equation describing heat flow into the hot side:

$$q_h = \alpha T_c I + \frac{1}{R_{\text{th}}}(T_c - T_h) + \frac{1}{2}R_{\text{el}}I^2 \quad (3)$$

As we are looking at the worst-case scenario, we assume that $T_c = T_h$ and the thermal conduction component goes away. The first component, representing q_{peb} can be set as the Q_{max} value of the specific TEM used. In our case, $Q_{max} = 1.7\text{W}$. The maximum current for our TEM is 0.7A, and its resistive load is 4.17Ω. As there are nine total TEMs in our assembly, $Q_{max_{Array}}$ can be calculated as:

$$Q_{max_{Array}} = 9 * (1.7 + \frac{1}{2}4.17 * 0.7^2) = 24.49W \quad (4)$$

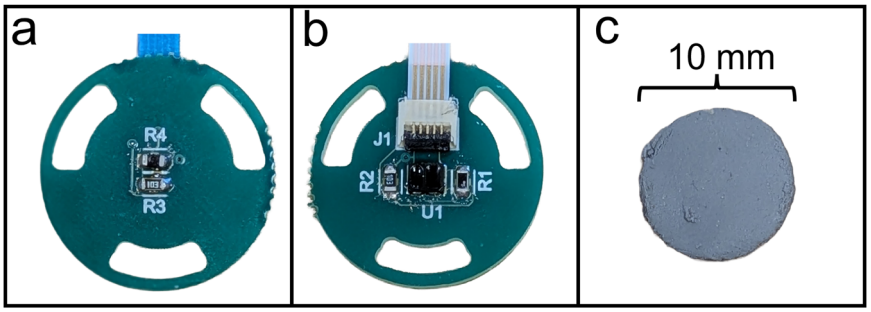


Fig. 9 | Surface contact and temperature measurement sensors. a An 0603 footprint 10k thermistor (R4) with voltage dividing resistor (R3) on the top (outward facing) surface of the sensing module. **b** A reflective phototransistor (U1) is mounted on the bottom surface of the module, facing inwards towards the silicone body of the haptic device. An initial air-gap of 0.5 mm is maintained between the phototransistor and the device's silicone body using 3M VHB 4905 double-sided tap as a spacer. When pressure is applied to a module during contact with a physical surface, this airgap is closed and the phototransitor changes state, signaling contact. **c** A 10 mm thermally conductive silicone pad is mounted on top of the temperature sensor to aid in even heat transfer and accurate temperature measurement of contact surfaces.

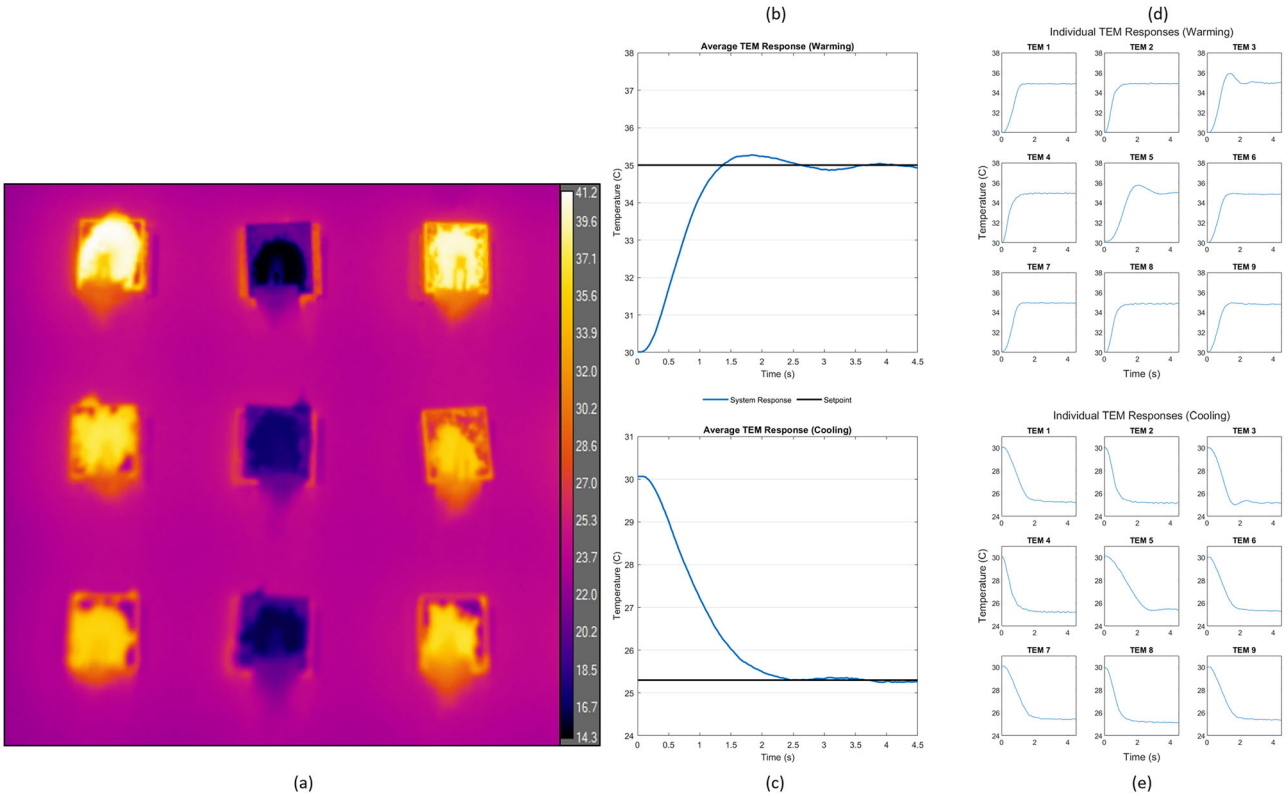


Fig. 10 | Thermal feedback device performance. a Each channel of the TEM array can be individually actuated, allowing for multiple spatial patterns to be formed and presented to the palm. Also shown in Fig. 2e. The average temperature response to a step input while in contact with a human palm for warming (**b**) and cooling (**c**) modes. Individual TEM responses for warming (**d**) and cooling (**e**) show that variance exists in an individual TEM's response, most likely due to variable contact pressure with the palm (and therefore variable rates of thermal transfer into the skin). Data for **b**–**e** available in Supplemental Data 1: TEM Response Times.

The maximum temperature rise for the water in the watercooling system can then be described by:

$$\Delta T = \frac{Q_{max_{Array}}}{\rho V c} \tag{5}$$

where ρ is the density of water ($1000\frac{kg}{m^3}$), V is the volumetric flowrate (measured to be $2.25\frac{ml}{s}$), and c is the specific heat of water ($4182\frac{J}{kg \cdot K}$). Plugging these values in we get a maximum temperature differential of:

$$\Delta T = \frac{24.49}{1000 * 2.25E^{-6} * 4184} = 2.60K \tag{6}$$

The intermittent use of the TEMS, combined with relatively small ΔT for the water and the relatively large size of our water reservoir, leads us to conclude that the water cooling system will remain stable even with prolonged use of the device.

A heating element within the water reservoir kept the water temperature at 30 °C, which is within the range of skin temperature of

25–36 °C[1,58]. Due to the large size of the water cooling channels compared to the size of the device, and the thermal properties of the silicone material with which it was made, this maintained a steady temperature of 30 °C for the entire thermal device. Maintaining the wearable thermal device at skin temperature is of great importance for multiple reasons. First and foremost, doing so establishes a neutral baseline, enabling the user to perceive both warming and cooling stimuli from the device. This neutral baseline also minimizes sensory adaptation, thereby preserving the sensitivity and responsiveness of the user's skin to the thermal haptic feedback. Additionally, keeping the device at skin temperature when not actively providing thermal feedback enhances user comfort and reduces the likelihood of skin irritation or discomfort from prolonged contact with a device that is either too cold or too warm.

Device performance

The PID gains were tuned by hand, with the same gains applied to each TEM subsystem. Investigating the dynamic performance of the device, a step input exhibited a quick response for both warming and cooling modes while in contact with a human palm. A warming rise time of 1.4 s and a cooling rise time of 2.4 s were observed (Fig. 10b–e). It is worth noting that the disparity in these rise times can be ascribed to the resistive heating of the TEMs, which facilitates the temperature increase in warming mode while impeding the temperature decrease in cooling mode.

Data availability

Source data for figures 2 and 10 are available as supplementary data in "Supplementary Data 1: TEM Response Times." Source data for Figures 3 and 6 and Tables 1, 3, 4, and 5 are available as supplementary data in "Supplementary Data 2: Human Subjects Data."

Code availability

All statistical analyses were conducted with Matlab 2026a. All statistical analysis code can be found in "Supplemental Data 3: Matlab Data Processing Code."

Received: 12 May 2025; Accepted: 12 October 2026;
Published online: 13 November 2026

References

1. Jones, L. A. & Berris, M. Material discrimination and thermal perception. In *Proc. 11th Symposium on Haptic Interfaces for Virtual Environment and Teleoperator Systems, HAPTICS 2003* 171–178 https://doi.org/10.1109/HAPTIC.2003.1191267 (2003).
2. Peiris, R. L., Peng, W., Chen, Z., Chan, L. & Minamizawa, K. ThermoVR: Exploring integrated thermal haptic feedback with head mounted displays. *Conf. Hum. Factors Comput. Syst. Proc.* **2017**, 5452–5456 https://doi.org/10.1145/3025453.3025824 (2017).
3. Gibbs, J. K., Gillies, M. & Pan, X. A comparison of the effects of haptic and visual feedback on presence in virtual reality. *Int. J. Hum. Comput. Stud.* **157**, 102717 https://doi.org/10.1016/j.ijhcs.2021.102717 (2022).
4. Lontschar, S., Deegan, D., Humer, I., Pietroszek, K. & Eckhardt, C. Analysis of haptic feedback and its influences in virtual reality learning environments. In *Proc. 2020 6th International Conference of the Immersive Learning Research Network (iLRN)*, 171–177 https://doi.org/10.23919/iLRN47897.2020.9155087 (2020).
5. John, B. & Wickramasinghe, N. A review of mixed reality in health care. in *Delivering Superior Health and Wellness Management with IoT and Analytics* (eds. Wickramasinghe, N. & Bodendorf, F.) 375–382 (Springer International Publishing, Cham, 2020) https://doi.org/10.1007/978-3-030-17347-0_18.
6. Santi, G. M., Ceruti, A., Liverani, A. & Osti, F. Augmented reality in industry 4.0 and future innovation programs. *Technologies* **9**, 33 https://doi.org/10.3390/technologies9020033 (2021).
7. Bazavan, L.-C., Roibu, H., Petcu, F. B., Cismaru, S. I. & George, B. N. Virtual reality and augmented reality in education. In *Proc. 2021 30th Annual Conference of the European Association for Education in Electrical and Information Engineering (EAEEIE)*, 1–4 https://doi.org/10.1109/EAEEIE50507.2021.9531005 (2021).
8. Sırakaya, M. & Alsancak Sırakaya, D. Augmented reality in STEM education: a systematic review. *Interact. Learn. Environ.* **30**, 1556–1569 https://doi.org/10.1080/10494820.2020.1722713 (2022).
9. Liberatore, M. J. & Wagner, W. P. Virtual, mixed, and augmented reality: a systematic review for immersive systems research. *Virtual Real.* **25**, 773–799 https://doi.org/10.1007/s10055-020-00492-0 (2021).
10. Akgün, M. & Atıcı, B. The effects of immersive virtual reality environments on students' academic achievement: a meta-analytical and meta-thematic study. *Particip. Educ. Res.* **9**, 111–131 https://doi.org/10.17275/per.22.57.9.3 (2022).
11. Guerra-Tamez, C. R. The impact of immersion through virtual reality in the learning experiences of art and design students: the mediating effect of the flow experience. *Educ. Sci.* **13**, 185 https://doi.org/10.3390/educsci13020185 (2023).
12. Milgram, P. & Kishino, F. A taxonomy of mixed reality visual displays. *IEICE Trans. Inf. Syst.* **77**, 1321–1329 (1994).
13. Azuma, R. T. A survey of augmented reality. *Presence* **6**, 355–385 (1997).
14. Apple Vision Pro. https://www.apple.com/apple-vision-pro/.
15. Garcia-Valle, G., Ferre, M., Brenosa, J. & Vargas, D. Evaluation of presence in virtual environments: haptic vest and user's haptic skills. *IEEE Access* **6**, 7224–7233 https://doi.org/10.1109/ACCESS.2017.2782254 (2017).
16. Krogmeier, C., Mousas, C. & Whittinghill, D. Human–virtual character interaction: toward understanding the influence of haptic feedback. *Comput. Animat. Virtual Worlds* **30**, e1883 https://doi.org/10.1002/cav.1883 (2019).
17. Richard, G., Pietrzak, T., Argelaguet, F., Lécuyer, A. & Casiez, G. Studying the role of haptic feedback on virtual embodiment in a drawing task. *Front. Virtual Real.* **1** (2021).
18. Basdogan, C., Ho, C. H., Srinivasan, M. A. & Slater, M. An experimental study on the role of touch in shared virtual environments. *ACM Trans. Comput. Hum. Interact.* **7**, 443–460 https://doi.org/10.1145/365058.365082 (2000).
19. Slater, M. & Sanchez-Vives, M. V. From presence to consciousness through virtual reality. *Nat. Rev. Neurosci.* **6**, 332–339 (2005).
20. Ho, H. N. Material recognition based on thermal cues: mechanisms and applications. *Temperature* **5**, 36–55 https://doi.org/10.1080/23328940.2017.1372042 (2018).
21. Cai, S., Ke, P., Narumi, T. & Zhu, K. ThermAirGlove: a pneumatic glove for thermal perception and material identification in virtual reality. In *Proc. 2020 IEEE Conference on Virtual Reality and 3D User Interfaces (VR)*, 248–257 (IEEE, 2020) https://doi.org/10.1109/VR46266.2020.00044.
22. Sun, Z., Zhu, M., Shan, X. & Lee, C. Augmented tactile-perception and haptic-feedback rings as human-machine interfaces aiming for immersive interactions. *Nat. Commun.* **13**, 5224. https://doi.org/10.1038/s41467-022-32745-8 (2022).
23. Oh, J. et al. A liquid metal based multimodal sensor and haptic feedback device for thermal and tactile sensation generation in virtual reality. *Adv. Funct. Mater.* **31**, 2007772 https://doi.org/10.1002/adfm.202007772 (2021).
24. Zhu, M. et al. Haptic-feedback smart glove as a creative human-machine interface (HMI) for virtual/augmented reality applications. *Sci. Adv.* **6**, eaaz8693 https://doi.org/10.1126/sciadv.aaz8693 (2020).
25. Huang, Y. et al. A skin-integrated multimodal haptic interface for immersive tactile feedback. *Nat. Electron.* **6**, 1020–1031 https://doi.org/10.1038/s41928-023-01074-z (2023).

26. Aziz, K. M. A. et al. Haptic handshank – a handheld multimodal haptic feedback controller for virtual reality. In *Proc. 2020 IEEE International Symposium on Mixed and Augmented Reality (ISMAR)*, 239–250 (IEEE, 2020) https://doi.org/10.1109/ISMAR50242.2020.00047.
27. Bhatia, A., Hornbæk, K. & Seifi, H. Augmenting the feel of real objects: An analysis of haptic augmented reality. *Int. J. Hum. Comput. Stud.* **185**, 103244 https://doi.org/10.1016/j.ijhcs.2024.103244 (2024).
28. Lederman, S. J. & Klatzky, R. L. Hand movements: A window into haptic object recognition. *Cogn. Psychol.* **19**, 342–368 https://doi.org/10.1016/0010-0285(87)90008-9 (1987).
29. Sanz Cozcolluela, A., Wösten, K. & Vardar, Y. Generating multimodal textures with a soft hydro-pneumatic haptic ring. *Int. J. Hum. Comput. Stud.* **212**, 103814 https://doi.org/10.1016/j.ijhcs.2026.103814 (2026).
30. Wang, H., Singhal, Y., Gil, H. & Kim, J. R. Fiery hands: designing thermal glove through thermal and tactile integration for virtual object manipulation. In *Proc. 37th Annual ACM Symposium on User Interface Software and Technology, UIST '24*, 1–15 (Association for Computing Machinery, New York, NY, USA, 2024) https://doi.org/10.1145/3654777.3676457.
31. Zhu, K., Perrault, S., Chen, T., Cai, S. & Lalintha Peiris, R. A sense of ice and fire: exploring thermal feedback with multiple thermoelectric-cooling elements on a smart ring. *Int. J. Hum. Comput. Stud.* **130**, 234–247 https://doi.org/10.1016/j.ijhcs.2019.07.003 (2019).
32. Peiris, R. L., Feng, Y.-L., Chan, L. & Minamizawa, K. ThermalBracelet: exploring thermal haptic feedback around the wrist. In *Proc. 2019 CHI Conference on Human Factors in Computing Systems*, 1–11 (ACM, New York, NY, USA, 2019) https://doi.org/10.1145/3290605.3300400.
33. Manasrah, A., Crane, N., Guldiken, R. & Reed, K. B. Perceived cooling using asymmetrically-applied hot and cold stimuli. *IEEE Trans. Hapt.* **10**, 75–83 https://doi.org/10.1109/TOH.2016.2578334 (2017).
34. Jones, L. A. & Ho, H. N. Warm or cool, large or small? The challenge of thermal displays. *IEEE Trans. Hapt.* **1**, 53–70 https://doi.org/10.1109/TOH.2008.2 (2008).
35. Filingeri, D., Zhang, H. & Arens, E. A. Thermosensory micromapping of warm and cold sensitivity across glabrous and hairy skin of male and female hands and feet. *J. Appl. Physiol.* **125**, 723–736 https://doi.org/10.1152/japplphysiol.00158.2018 (2018).
36. Caldwell, D. G., Tsagarakis, N. & Wardle, A. Mechano thermo and proprioceptor feedback for integrated haptic feedback. *Proc. IEEE Int. Conf. Robot. Autom.* **3**, 2491–2496 https://doi.org/10.1109/robot.1997.619335 (1997).
37. Hirai, S. & Miki, N. A Thermal Tactile Sensation Display with Controllable Thermal Conductivity. *Micromachines* **10**, 359 https://doi.org/10.3390/mi10060359 (2019).
38. Lee, J. et al. Stretchable skin-like cooling/heating device for reconstruction of artificial thermal sensation in virtual reality. *Adv. Funct. Mater.* **30**, 1909171 https://doi.org/10.1002/adfm.201909171 (2020).
39. Green, B. G. Localization of thermal sensation: an illusion and synthetic heat. *Percept. Psychophys.* **22**, 331–337 https://doi.org/10.3758/BF03199698 (1977).
40. Singhal, Y., Honrales, D., Wang, H. & Kim, J. R. Thermal in motion: designing thermal flow illusions with tactile and thermal interaction. In *Proc. 37th Annual ACM Symposium on User Interface Software and Technology, UIST '24*, 1–13 (Association for Computing Machinery, New York, NY, USA, 2024) https://doi.org/10.1145/3654777.3676460.
41. Liu, Y., Nishikawa, S., ah Seong, Y., Niiyama, R. & Kuniyoshi, Y. ThermoCaress: a wearable haptic device with illusory moving thermal stimulation. In *Proc. 2021 CHI Conference on Human Factors in Computing Systems*, 1–12 (ACM, New York, NY, USA, 2021) https://doi.org/10.1145/3411764.3445777.
42. Son, H., Wang, H., Singhal, Y. & Kim, J. R. Upper body thermal referral and tactile masking for localized feedback. *IEEE Trans. Vis. Comput. Graph.* **29**, 2211–2219 https://doi.org/10.1109/TVCG.2023.3247068 (2023).
43. Nakatani, M. et al. A novel multimodal tactile module that can provide vibro-thermal feedback. in *Haptic Interaction, Lecture Notes in Electrical Engineering* (eds Hasegawa, S., Konyo, M., Kyung, K.-U., Nojima, T. & Kajimoto, H.) 437–443 (Springer, Singapore, 2018) https://doi.org/10.1007/978-981-10-4157-0_73.
44. Zhang, J., Li, H., Song, A., Ding, Y. & Wu, J. Thermal perception for information transmission: theoretical analysis, device design, and experimental verification. *IEEE Trans. Hapt.* **15**, 679–692 https://doi.org/10.1109/TOH.2022.3208937 (2022).
45. Zhipeng, M. et al. A thermal tactile display device with multiple heat sources. In *Proc. 2012 International Conference on Industrial Control and Electronics Engineering*, 192–195 https://doi.org/10.1109/ICICEE.2012.58 (2012).
46. Li, H. et al. Muscle temperature sensing and control with a wearable device for hand rehabilitation of people after stroke. In *Proc. 2020 International Conference on Sensing, Measurement & Data Analytics in the Era of Artificial Intelligence (ICSMD)*, 94–99 https://doi.org/10.1109/ICSMD50554.2020.9261634 (2020).
47. Kim, S. et al. Two-dimensional thermal haptic module based on a flexible thermoelectric device. *Soft Robot.* **7**, 736–742 https://doi.org/10.1089/soro.2019.0158 (2020).
48. Yarnitsky, D. & Ochoa, J. L. Warm and cold specific somatosensory systems: psychophysical thresholds, reaction times and peripheral conduction velocities. *Brain* **114**, 1819–1826 https://doi.org/10.1093/brain/114.4.1819 (1991).
49. Kenshalo, D. R., Holmes, C. E. & Wood, P. B. Warm and cool thresholds as a function of rate of stimulus temperature change. *Percept. Psychophys.* **3**, 81–84 https://doi.org/10.3758/BF03212769 (1968).
50. Kingdom, F. & Prins, N. Adaptive methods. in *Psychophysics: A Practical Introduction* 2 edn (Elsevier Science & Technology).
51. Hojatmadani, M., Rigsby, B. & Reed, K. B. Time delay affects thermal discrimination. *IEEE Trans. Hapt.* **15**, 451–457 https://doi.org/10.1109/TOH.2022.3156122 (2022).
52. Yang, G.-H., Kyung, K.-U., Srinivasan, M. & Kwon, D.-S. Quantitative tactile display device with pin-array type tactile feedback and thermal feedback. In *Proc. 2006 IEEE International Conference on Robotics and Automation, ICRA*. 3917–3922 https://doi.org/10.1109/ROBOT.2006.1642302 (2006).
53. Jung, Y. et al. High heat storing and thermally diffusive artificial skin for wearable thermal management. *Nano Energy* **105**, 107979 https://doi.org/10.1016/j.nanoen.2022.107979 (2023).
54. Luo, Y. et al. Flexible liquid metal-based microfluidic strain sensors with fractal-designed microchannels for monitoring human motion and physiological signals. *Biosens. Bioelectron.* **246**, 115905 https://doi.org/10.1016/j.bios.2023.115905 (2024).
55. Chen, F., Nilsson, H. & Holmér, I. Finger cooling by contact with cold aluminium surfaces — effects of pressure, mass and whole body thermal balance. *Eur. J. Appl. Physiol. Occup. Physiol.* **69**, 55–60 https://doi.org/10.1007/BF00867928 (1994).
56. Rykaczewski, K. Modeling thermal contact resistance at the finger-object interface. *Temperature* **6**, 85–95 https://doi.org/10.1080/23328940.2018.1551706 (2019).
57. Tiest, W. M. An experimentally verified model of the perceived 'coldness' of objects. In *Proc. Second Joint EuroHaptics Conference and Symposium on Haptic Interfaces for Virtual Environment and Teleoperator Systems, World Haptics 2007* 61–65 https://doi.org/10.1109/WHC.2007.21 (2007).
58. Verrillo, R., Bolanowski, S., Francis, C. & McGlone, F. Effects of hydration on tactile sensation. *Somatosens. Mot. Res.* **15**, 93–108 https://doi.org/10.1080/08990229870826 (1998).

Author contributions

A.W., R.G., and N.S. conceptualized and designed the research. A.W., E.C., and R.G. designed and built the experimental hardware and conducted the experiment. A.W. and N.S. analyzed the data. A.W. wrote the manuscript and prepared figures. All authors reviewed the manuscript.

Funding

We gratefully acknowledge the support provided for this research by the National Science Foundation under the award 2225890. The content is solely the responsibility of the authors and does not necessarily represent the official views of the National Science Foundation.

Competing interests

The authors declare no competing interests.

Additional information

Supplementary information The online version contains supplementary material available at https://doi.org/10.1038/s44172-026-00817-y.

Correspondence and requests for materials should be addressed to Alexandra Watkins.

Peer review information *Communications Engineering* thanks all reviewer(s) for their contribution to the peer review of this work. Primary Handling Editors: [Philip Coatsworth]. A peer review file is available.

Reprints and permissions information is available at http://www.nature.com/reprints

Publisher's note Springer Nature remains neutral with regard to jurisdictional claims in published maps and institutional affiliations.

Open Access This article is licensed under a Creative Commons Attribution-NonCommercial-NoDerivatives 4.0 International License, which permits any non-commercial use, sharing, distribution and reproduction in any medium or format, as long as you give appropriate credit to the original author(s) and the source, provide a link to the Creative Commons licence, and indicate if you modified the licensed material. You do not have permission under this licence to share adapted material derived from this article or parts of it. The images or other third party material in this article are included in the article's Creative Commons licence, unless indicated otherwise in a credit line to the material. If material is not included in the article's Creative Commons licence and your intended use is not permitted by statutory regulation or exceeds the permitted use, you will need to obtain permission directly from the copyright holder. To view a copy of this licence, visit http://creativecommons.org/licenses/by-nc-nd/4.0/.

© The Author(s) 2026

This Article in Press is shared early to give you faster access to new research. It is citable and carries a permanent DOI. The final edited version will replace it automatically.